Int. J. Heat Mass Transfer. Vol. 35, No. 5, pp. 1069–1076, 1992
Printed in Great Britain

0017–9310/92 $5.00+0.00

Convection in a differentially-heated square cavity with a torsionally-oscillating lid

REIMA IWATSU
Institute of Computational Fluid Dynamics, 1-22-3 Haramachi, Meguro, Tokyo 152, Japan

JAE MIN HYUN
Korea Advanced Institute of Science and Technology, P.O. Box 150, Cheongryang, Seoul, Korea

and

KUNIO KUWAHARA
The Institute of Space and Astronautical Science, Yoshinodai, Sagamihara, Kanagawa, Japan

(*Received* 5 *March* 1991 *and in final form* 28 *May* 1991)

Abstract—Numerical studies are made of the flow of a viscous thermally-stratified fluid in a square container. The flow is driven by the top lid of the container, which executes torsional oscillations. A stabilizing vertical temperature difference ($T_H - T_C$) is applied on the horizontal boundary walls; the two vertical side walls are thermally insulated. Numerical solutions are secured to the time-dependent Navier–Stokes equations under the Boussinesq-fluid approximation. Details of unsteady flow and thermal fields are exhibited over broad ranges of three principal parameters, i.e. the Reynolds number *Re*, the Grashof number *Gr*, and the frequency ratio ω'. Of particular interest is the possibility of resonance; this gives rise to intensification of flows in the interior and associated augmentation of convective heat transport. Systematically-organized computational results indicate that the existence of resonance is verified, and the enhancement of heat transfer is demonstrated at particular values of ω'.

1. INTRODUCTION

THE FLOW of an incompressible viscous fluid, of kinematic viscosity ν, in a closed cavity poses a classical problem. The basic configuration consists of the flow in a square cavity of size L; the flow is driven by the top lid which slides at uniform speed U_0 in its own plane. The geometry is simple and the boundary conditions are regular; this flow has served as a benchmark for numerical as well as experimental model validations. The major characteristics have been clearly identified and plausible physical explanations have been rendered for this flow model [1–14] over a broad range of the Reynolds number $Re \equiv U_0 L/\nu$.

The unsteady driven-cavity flows have received relatively little attention, although unsteady flows are of frequent occurrence in engineering applications.

The flow properties developed in the cavity when the sliding lid executes a torsional oscillation, $u = U_0 \sin \omega t$, present a canonical model for unsteady driven-cavity problems. In this case, the frequency parameter, $\omega' = \omega/(U_0/L)$, emerges to be a principal non-dimensional parameter, in addition to the above-defined Reynolds number.

Some of the basic features of this particular unsteady flow were explored recently by Soh and Goodrich [15]. However, the primary purpose of Soh and Goodrich was to establish the computational validity of a new numerical scheme by using this unsteady flow as an example. Iwatsu *et al.* [16] provided a comprehensive numerical solution to the full time-dependent Navier–Stokes equations in order to illuminate the prominent characteristics of this unsteady driven-cavity flow. It was shown that the overall flow properties display marked qualitative differences as the two governing parameters, *Re* and ω', encompass wide ranges. In the low-frequency regime (ω' small), much of the flow in the bulk of the cavity is affected by the torsional oscillation of the lid. On the contrary, when ω' is large, the fluid motion is confined to a narrow layer adjacent to the oscillating lid. When ω' is intermediate, the effect of the confining side walls is pronounced; in this regime, significant changes are discernible between the low-*Re* and high-*Re* limits. The numerical solutions of Iwatsu *et al.* [16] laid groundwork to comprehend the fundamental dynamics pertinent to the unsteady flows of this class.

In this paper, it is proposed that the aforementioned unsteady driven-cavity flow model is extended to include the buoyancy effect. In general, buoyancy inhibits vertical motions; therefore, the global flow patterns will be substantially affected by the buoyancy effect. From the standpoint of practical engineering applications, the introduction of buoyancy brings the analysis closer to realistic systems. Specifically, the flow configuration is such that the oscillating lid is maintained at temperature T_H, and the temperature at the bottom wall is T_C, $T_H > T_C$; this creates a stably

NOMENCLATURE

g	gravitational acceleration	T_H	temperature of the top lid
Gr	Grashof number, $g\alpha(T_H-T_C)L^3/\nu^2$	U_0	maximum speed of the top lid motion
H_x	heat flux in the x-direction (see equation (4))	$\mathbf{V}$	velocity vector, (u, v)
H_y	heat flux in the y-direction (see equation (5))	x	horizontal coordinate (see Fig. 1)
L	depth (width) of the cavity	y	vertical coordinate (see Fig. 1).
N	Brunt–Väisälä frequency, $[\alpha g(T_H-T_C)/L]^{1/2}$	Greek symbols	
p	pressure	α	coefficient of thermometric expansion
Pr	Prandtl number, ν/κ	κ	thermal conductivity
Re	Reynolds number, U_0L/ν	ν	kinematic viscosity of the fluid
T	temperature	ω	frequency of the torsional oscillation of the top lid
T_C	temperature of the bottom wall	ω'	frequency parameter, $\omega L/U_0$.

stratified fluid system. The side walls are thermally insulated.

The introduction of the buoyancy effect is characterized by the Grashof number, $Gr = g\alpha(T_H - T_C)L^3/\nu^2$, where g is the acceleration due to gravity and α the coefficient of thermometric expansion. The objective of the present analysis is to examine the flow and heat transfer characteristics of this unsteady stratified fluid system. This has practical implications. It is well known that the heat transfer of a confined fluid system can be greatly augmented by inducing convective activities; by this method, the heat transfer rates at the surface walls can exceed the values obtainable by the conductive mode alone. In other words, the present study is also motivated by the possibility of heat transfer enhancement in the cavity by forcing the top lid to oscillate at an appropriate frequency.

The strength of a stratified fluid is often measured by the Brunt–Väisälä frequency, $N = [\alpha g(T_H - T_C)/L]^{1/2}$, which represents one natural frequency of the physical system. A perusal of the problem formulation suggests a possible resonance when the values of the externally-forced frequency ω and the natural frequency of the system are related to each other. When such resonance phenomena are indeed realized, convective flows are intensified and, consequently, the accompanying heat transfer augmentation may be materialized.

In the present work, extensive numerical solutions are acquired to the unsteady driven-cavity flows when a vertically-stabilizing temperature gradient is imposed. It is shown explicitly that both the flow and heat transfer characteristics are substantially altered when ω takes values such that resonance can be expected in this stratified fluid system. The wealth of numerical data permits a systematic evaluation of flow intensification and heat transfer augmentation as ω' covers a broad range. The present investigation intends to demonstrate, by resorting to numerical simulations, heat transfer enhancement in a confined cavity. The results of the numerical solutions clearly point to the fact that, at high Grashof numbers, heat transfer rates can be substantially increased by choosing a proper value of ω such that the resonance conditions are satisfied. These findings are qualitatively consistent with the elementary physical argument.

2. NUMERICAL MODEL

The basic equations are the Navier–Stokes equations with the Boussinesq-fluid assumption and the energy equation. These can be expressed in non-dimensional form as

$$\operatorname{div} \mathbf{V} = 0 \tag{1}$$

$$\frac{\partial \mathbf{V}}{\partial t} + (\mathbf{V}\cdot\operatorname{grad})\mathbf{V} = -\operatorname{grad} p + Re^{-1}\Delta\mathbf{V} + Gr\cdot Re^{-2}\,T\mathbf{e} \tag{2}$$

$$\frac{\partial T}{\partial t} + (\mathbf{V}\cdot\operatorname{grad})T = (Pr\cdot Re)^{-1}\Delta T \tag{3}$$

where $\mathbf{e} = (0, -1)$, $\mathbf{V} = (u, v)$ is the velocity vector, p the pressure and T the temperature. In the above, non-dimensionalizations were implemented by using L, U_0, L/U_0, and $(T_H - T_C)$ for reference scales for length, velocity, time, and temperature, respectively. The differential operators are

$$\operatorname{div}\mathbf{V} = \frac{\partial u}{\partial x} + \frac{\partial v}{\partial y}, \quad \operatorname{grad} = \left(\frac{\partial}{\partial x}, \frac{\partial}{\partial y}\right),$$

$$\Delta = \operatorname{div}\cdot\operatorname{grad}.$$

The numerical model is a modified version of the MAC method [17], with a third-order upwind scheme applied to the non-linear terms [18]. Particular attention is given to the choice of difference schemes for div, grad and Δ (scheme 2 of ref. [19] is adopted). The

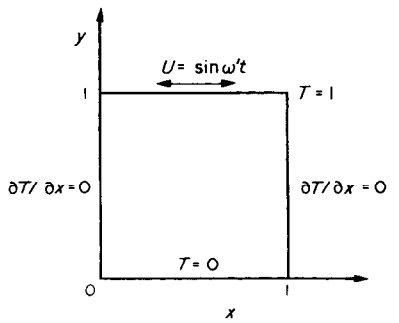

FIG. 1. The flow configuration and the coordinate system.

temperature equation is discretized in accordance with the control volume technique.

The flow configuration and the associate boundary conditions are depicted in Fig. 1. The boundary conditions are

$$\mathbf{V} = (\sin(\omega' t), 0) \quad \text{at} \quad y = 1, 0 \leqslant x \leqslant 1$$

$$\mathbf{V} = 0 \quad \text{at} \quad x = 0, 1, 0 \leqslant y \leqslant 1$$

$$\text{and} \quad y = 0, 0 \leqslant x \leqslant 1$$

$$T = 0 \quad \text{at} \quad y = 0, 0 \leqslant x \leqslant 1$$

$$T = 1 \quad \text{at} \quad y = 1, 0 \leqslant x \leqslant 1$$

$$\frac{\partial T}{\partial x} = 0 \quad \text{at} \quad x = 0 \quad \text{and} \quad x = 1.$$

As is evident in the foregoing formulation, the problem is characterized by the following four principal dimensionless numbers: the Reynolds number, $Re = U_0 L/\nu$; the frequency parameter $\omega' = \omega/(U_0/L)$; the Grashof number, $Gr = g\alpha(T_H - T_C)L^3/\nu^2$; and the Prandtl number, $Pr = \nu/\kappa$.

3. RESULTS

Complete calculations have been made for a total of 40 cases. Three specific values of Re were chosen: $Re = 400$, 1000 and 2000. The range of Gr was $Gr = 0$ to 10^6; the values of ω' were $0.1 \leqslant \omega' \leqslant 10.0$. The Prandtl number was fixed at $Pr = 0.71$.

The numbers of grid points were 65×65 and 129×129 for the cases of $Re = 400$, and $Re = 1000$ and 2000, respectively; the time interval Δt was taken as either $(2\pi/\omega')/1000$ or $(2\pi/\omega')/4000$. These were supposed to provide sufficient resolution to the numerical results. The typical CPU time per case of computation was about 10 min to 2 h on the VP-200/400 super-computer system.

Several test calculations have been made in order to appraise the reliability and accuracy of the present numerical solutions. Computations were carried out to reproduce the sample results obtained by Soh and Goodrich [15]; these efforts demonstrated close agreement between the present results and the solutions of Soh and Goodrich. The grid-dependency of the numerical results has been assessed systematically.

In the actual implementations of the numerical computations, at the initial state, the fluid was motionless and the linear temperature stratification ($T = y$) prevailed throughout the whole domain. Calculations were carried out, marching in time, until a sufficient number of quasi-periodic cycles were repeated. In most cases, the quasi-periodic steady-state, having the frequency of the forcing frequency, ω, was attained about three to six cycles after the initiation of the flow. The computed flow maintained high degrees of cyclic regularity after the quasi-periodic steady-state was reached. In the present results, typically about 20 cycles were computed in the quasi-periodic steady-state. The transitory approach to the establishment of the quasi-periodic state is not of primary concern in the present account.

The grid-convergence tests, both in space and time, have been performed by employing several different mesh networks. The outcome of these elaborate sensitivity tests to the grid proved to be highly satisfactory. For instance, at $Re = 1000$, the discrepancy in the results obtained by using the grids (129×129) and (257×257), was smaller than 0.1% (see Iwatsu *et al.* [16]). Based on extensive test calculations, the present numerical method is believed to possess high degrees of accuracy and reliability.

First, the effect of buoyancy is scrutinized. In general, the role of buoyancy is to inhibit vertical motions of a stratified fluid system. Figure 2 clearly exemplifies this trend, showing the profiles of the vertical velocities along the mid-height ($y = 0.5$). The suppression of vertical velocities is apparent as Gr increases. In general, the effect of buoyancy, relative to the forced convection stemming from the lid oscillation, can be measured by Gr/Re^2. The inhibition of vertical velocities for $Gr = 10^4$ is not noticeable; in this case, Gr/Re^2 is small, and the overall impact of buoyancy is still minor. The weakening of the vertical motions due to buoyancy is evident for higher values of Re (see, e.g. Fig. 3 for $Re = 10^3$).

Now, let us turn to the question of the effect of the frequency parameter, ω'. For an unstratified system ($N = 0$, $Gr = 0$), Iwatsu *et al.* [16] asserted that the global flow structure depends crucially on the frequency parameter. When ω' is very small, the bulk of the interior flow field is influenced by the oscillatory motion of the top lid. On the contrary, when ω' is large, the lid motion affects only the fluid confined in a shallow layer adjacent to the top lid. In the present problem of a stratified fluid system, much of the above statement is equally applicable in a qualitative sense. However, in the present system, the fluid is stratified [20, 21]; this implies that the system can support internal gravity waves with the characteristic frequency of $O(N)$. It is recalled that the present system is viscous and non-linear; therefore, the determination of the precise characteristic system frequency cannot readily be made a priori. However, when the frequency of the external excitation, ω, is close to the characteristic system frequency $O(N)$, it is expected that the interior

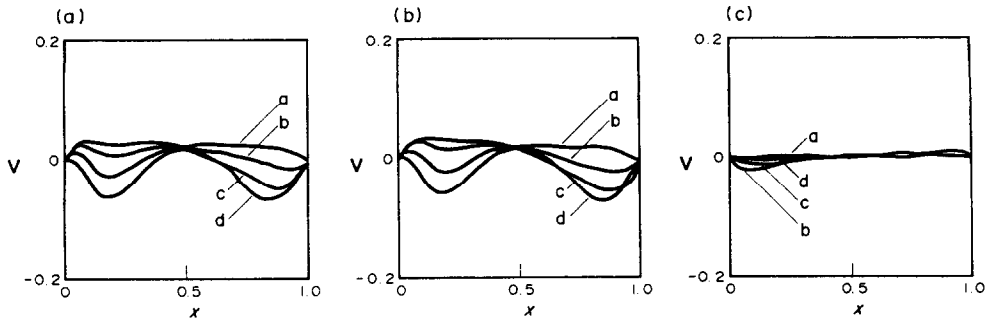

FIG. 2. Profiles of vertical velocity v along the horizontal mid-height, $y = 0.5$, during a half cycle of lid-oscillation. $Re = 400$, $\omega' = 1.0$. Times are: (a) 0; (b) $\tau/8$; (c) $\tau/4$; (d) $3\tau/8$; where τ is the period of lid-oscillation, $\tau = 2\pi/\omega'$. (a) $Gr = 0$, (b) $Gr = 10^4$, (c) $Gr = 10^6$.

fluid motions will be amplified, and the associated convective heat transfer will be augmented. This phenomenon is conveniently termed resonance.

In order to delineate this point, the heat transport across the sections of the cavity is plotted in Figs. 4 and 5. In Fig. 4, the profiles of the heat flux in the x-direction

$$H_x(x,t) \equiv \int_{y=0}^{y=1} \left(-Pr\ Re \cdot uT + \frac{\partial T}{\partial x} \right) dy \qquad (4)$$

are displayed. As is discernible, over much of the range of ω', the overall heat transport in the x-direction is largely contributed by the convection mode. It should be stressed that, as exemplified in Fig. 4(d), when $\omega' \sim 2.0$, heat transport is enhanced substantially; the augmentation of convective heat transport is apparent around this value of ω', indicating the possibility of resonance. It is noteworthy that, as depicted in Fig. 4(f), when ω' is very high, the excitation of fluid motions by the oscillating top lid is confined to a narrow layer close to the top lid. In this case, in the bulk of the interior region, the fluid is substantially motionless and the deviation of the temperature distributions from the original, conduction-dominant vertically-linear profile is minor. It follows that heat transfer becomes rather ineffective, and Fig. 4(f) bears out this point.

Similar, but more convincing, observations can be made in Fig. 5. In a manner analogous to (5), the overall heat transport in the y-direction can be measured

$$H_y(y,t) \equiv \int_{x=0}^{x=1} \left[-Pr\ Re \cdot vT + \frac{\partial T}{\partial y} \right] dx. \qquad (5)$$

As stressed previously, when ω' is small (see Fig. 5(a)), the bulk of the interior fluid is appreciably affected by the motion of the top lid. The convective heat transport is noticeable in much of the entire cavity. In the other extreme case of large ω' limit, the flow is confined into a narrow zone adjacent to the top lid. As ascertained in the above, H_y is close to unity (see Fig. 5(f)) in the majority of the cavity interior. The above observations concerning the flow structure are qualitatively consistent with the general behavior of the non-stratified fluid system reported earlier (see Iwatsu *et al.* [16]). However, for the present stratified system, the occurrence of resonance is notable. Figure 5(d), for $\omega' \sim 2.0$, demonstrates that, for this particular set of parameters, heat transport is substantially enhanced. This enhancement results

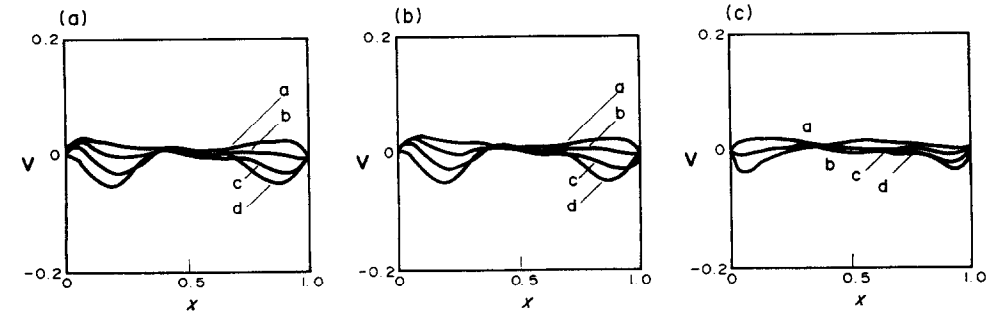

FIG. 3. Same as in Fig. 2, except $Re = 1000$. (a) $Gr = 0$, (b) $Gr = 10^4$, (c) $Gr = 10^6$.

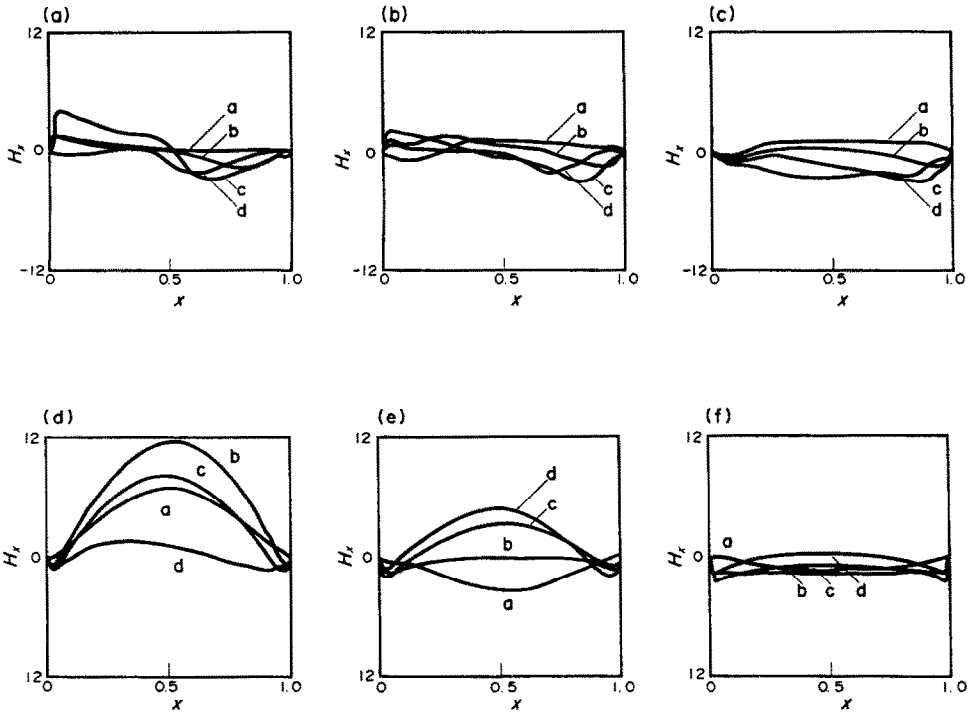

FIG. 4. Profiles of H_x, during a half cycle of lid-oscillation. $Re = 1000$, $Gr = 10^6$. Times are: (a) 0; (b) $\tau/8$; (c) $\tau/4$; (d) $3\tau/8$; where τ is the period of lid-oscillation, $\tau = 2\pi/\omega'$. (a) $\omega' = 0.1$, (b) $\omega' = 0.5$, (c) $\omega' = 1.0$, (d) $\omega' = 2.0$, (e) $\omega' = 3.0$, (f) $\omega' = 10.0$.

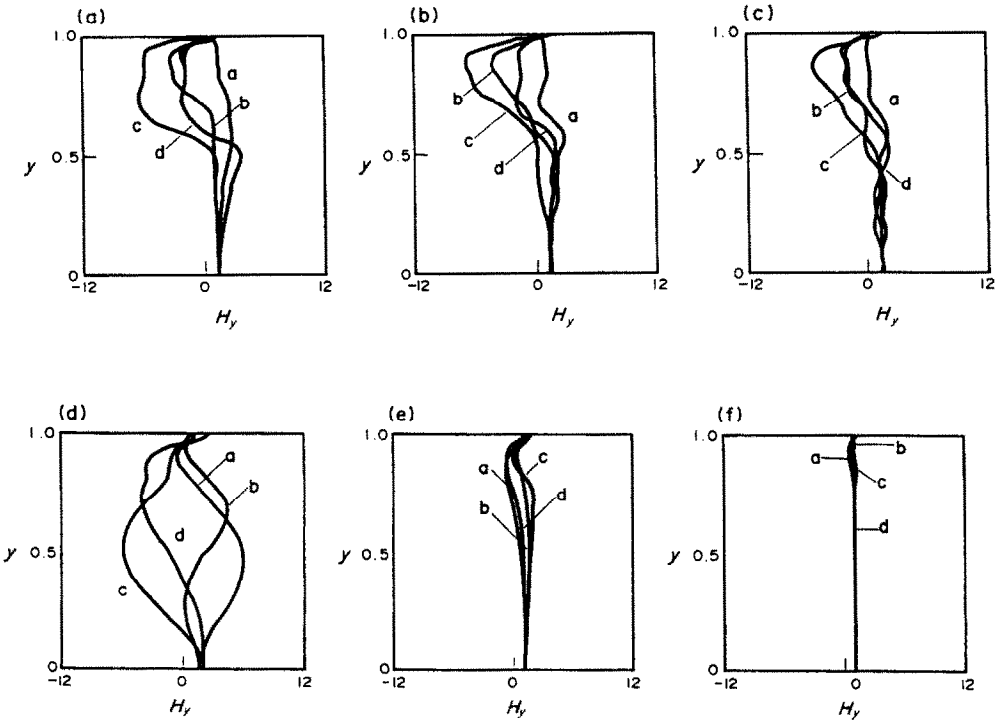

FIG. 5. Profiles of H_y, during a half cycle of lid-oscillation. $Re = 1000$, $Gr = 10^6$. Times are: (a) 0; (b) $\tau/8$; (c) $\tau/4$; (d) $3\tau/8$; where τ is the period of lid-oscillation, $\tau = 2\pi/\omega'$. (a) $\omega' = 0.1$, (b) $\omega' = 0.5$, (c) $\omega' = 1.0$, (d) $\omega' = 2.0$, (e) $\omega' = 3.0$, (f) $\omega' = 10.0$.

from the intensification of convective activities. These findings provide evidence that the overall heat transfer across the system boundaries can indeed be enhanced greatly by choosing appropriate values of the frequency of the external excitations.

The intensification of the flow due to resonance at particular frequencies can also be appreciated by inspecting the velocity data. Figure 6 summarizes the results of the entire set of computations. The purpose of these calculations is to detect the existence of resonance at particular values of the frequency parameter ω'. It is clear in Fig. 6 that $|v|_{\max}$, representing the amplification of the interior flows, peaks only at certain particular value(s) of ω'.

For the problem in hand, by undergoing elaborate numerical computations, the value(s) of ω' for resonance are searched for the given parameters, as demonstrated in Fig. 6. This will, in turn, indicate the ratio N/ω for resonance for that particular system under consideration. This information will be useful for system designers with a view toward maximizing the convective heat transport deliverable in the system.

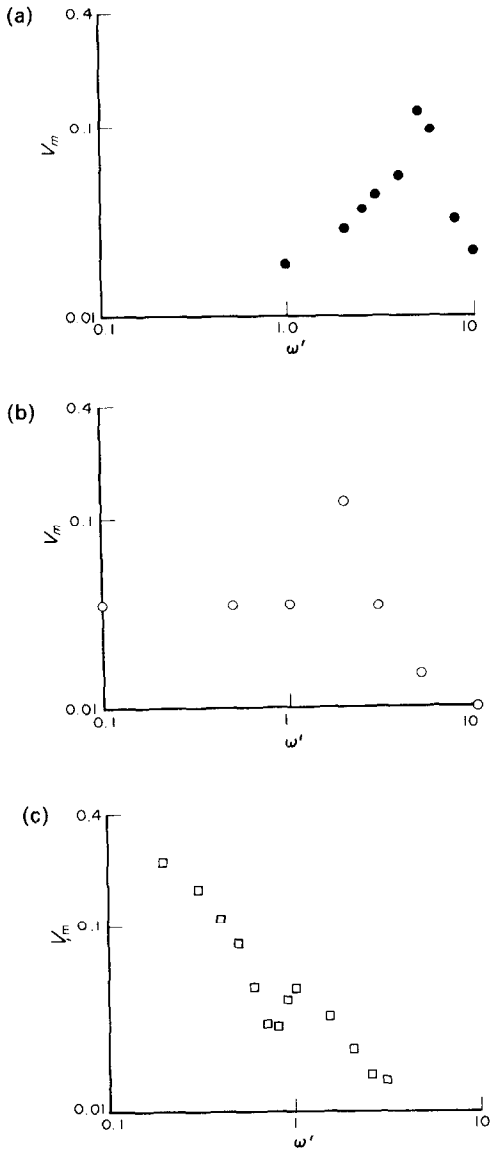

FIG. 6. Variations of the magnitude of maximum vertical velocity, $V_m \equiv \max|v|_{y=0.5}$, with ω'. (a) $Re = 400$, $Gr = 10^6$; (b) $Re = 1000$, $Gr = 10^6$; (c) $Re = 2000$, $Gr = 10^6$.

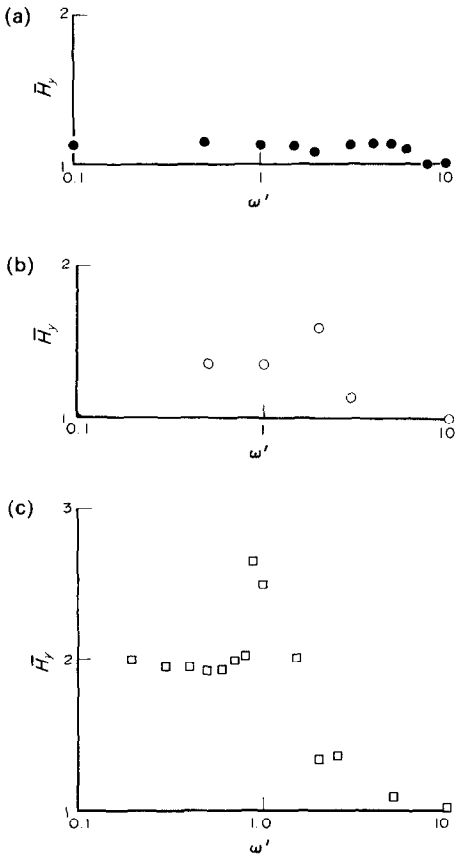

FIG. 7. Variations of the Nusselt number averaged over one cycle, $\bar{H}_y$, at the top lid ($y = 1.0$) with ω'. (a) $Re = 400$, $Gr = 10^6$; (b) $Re = 1000$, $Gr = 10^6$; (c) $Re = 2000$, $Gr = 10^6$.

The existence of resonance can also be inferred by the heat transfer data. Figure 7 illustrates the behavior of time-averaged heat transport, $\bar{H}_y$, at the top horizontal wall. It is clear, by inspecting Fig. 7, that substantial heat transfer augmentations are noticeable at selected values of ω'.

As emphasized earlier, since the system under consideration is highly non-linear and viscous, a priori determination of (N/ω) for resonance cannot be readily made. However, by plausible physically insightful reasoning, certain qualitative trends can be detected. Based on the original definitions, it can be rewritten that

$$Gr = (N/\omega)^2 Pr \cdot Re^2 \omega'^2. \tag{6}$$

If the system were strictly inviscid and linear, resonance would be expected at $N/\omega = 1.0$ and at higher harmonics. However, in the present realistic system, the maximum temperature difference achievable within the essentially inviscid interior region in the

cavity is smaller than $(T_H - T_C)$. Consequently, for practical systems, the value of ω' for resonance will be slightly larger than ω'_0 which would be obtained from equation (6) by setting $(N/\omega) = 1.0$. The numerical results illuminated in Figs. 6 and 7 are supportive of this relatively simple physical reasoning.

In the present work, due to the limitations of computer resources, two-dimensional flows have been treated. This will depict the eminent qualitative features germane to the cavity flows envisioned in the present paper. However, in an effort to simulate more realistic systems, calculations will be obtained of three-dimensional flows. The results of these endeavors will be reported in subsequent papers.

4. CONCLUSION

The introduction of stable stratification suppresses vertical motions. The present results illustrate that vertical motions weaken as Gr/Re^2 increases.

When the frequency parameter ω' is small, the bulk of the cavity interior is affected by the oscillation of the top lid. On the contrary, when ω' is large, flows are confined to a thin layer adjacent to the top lid. The vertical heat transfer in the interior is mostly conductive if $\omega' \gg 1$.

The present numerical data exhibited occurrence of resonance phenomena when the top lid oscillates at particular values of frequency. When the imposed frequency of the oscillating lid is close to these values, the fluid motion is amplified and the heat transfer across the system boundaries is enhanced.

The numerical results are qualitatively consistent with a fundamental physical argument.

REFERENCES

1. R. D. Mills, Numerical solutions of the viscous equations for a class of closed flows, *J. R. Aeronaut. Soc.* **69,** 714–718 (1965).
2. O. R. Burggraf, Analytical and numerical studies of structure of steady separated flows, *J. Fluid Mech.* **24,** 113–151 (1966).
3. F. Pan and A. Acrivos, Steady flows in rectangular cavities, *J. Fluid Mech.* **28,** 643–655 (1967).
4. J. D. Bozeman and C. Dalton, Numerical study of viscous flow in a cavity, *J. Comput. Phys.* **12,** 348–363 (1973).
5. S. Ozawa, Numerical studies of steady flow in a two-dimensional square cavity at high Reynolds numbers, *J. Phys. Soc. Japan* **38,** 889–895 (1975).
6. S. Y. Tuann and M. D. Olson, Review of computing methods for recirculating flows, *J. Comput. Phys.* **29,** 1–19 (1978).
7. A. S. Benjamin and V. E. Denny, On the convergence of numerical solutions for 2-D flows in a cavity at large *Re*, *J. Comput. Phys.* **33,** 340–358 (1979).
8. U. Ghia, K. N. Ghia and C. T. Shin, High-*Re* solutions for incompressible flow using the Navier–Stokes equations and a multigrid method, *J. Comput. Phys.* **48,** 387–411 (1982).
9. R. Schreiber and H. B. Keller, Driven cavity flows by efficient numerical technique, *J. Comput. Phys.* **49,** 310–333 (1983).
10. J. R. Koseff and R. L. Street, Visualization studies of a shear driven three-dimensional recirculation flow, *J. Fluids Engng* **106,** 21–29 (1984).
11. J. R. Koseff and R. L. Street, On end wall effects in a lid-driven cavity flow, *J. Fluids Engng* **106,** 385–389 (1984).
12. J. R. Koseff and R. L. Street, The lid-driven cavity flow: a synthesis of qualitative and quantitative observations, *J. Fluids Engng* **106,** 390–398 (1984).
13. R. Iwatsu, K. Ishii, T. Kawamura, K. Kuwahara and J. M. Hyun, Numerical simulation of three-dimensional flow structure in a driven-cavity, *Fluid Dyn. Res.* **5,** 173–189 (1989).
14. R. Iwatsu, J. M. Hyun and K. Kuwahara, Analyses of three-dimensional flow calculations in a driven cavity, *Fluid Dyn. Res.* **6,** 91–102 (1990).
15. W. H. Soh and J. W. Goodrich, Unsteady solution of incompressible Navier–Stokes equations, *J. Comput. Phys.* **79,** 113–134 (1988).
16. R. Iwatsu, J. M. Hyun and K. Kuwahara, Numerical simulation of torsionally-oscillating lid in a square cavity, to appear in *ASME J. Fluids Engng.*
17. F. H. Harlow and J. E. Welch, Numerical calculation of time-dependent viscous incompressible flow of fluid with free surface, *Physics Fluids* **8,** 2182–2187 (1965).
18. K. Kawamura and K. Kuwahara, Computation of high Reynolds number flow around a circular cylinder with surface roughness, AIAA paper 84-0340 (1984).
19. A. B. Stephens, J. B. Bell, J. M. Solomon and L. B. Hackerman, A finite difference Galerkin formulation for the incompressible Navier–Stokes equations, *J. Comput. Phys.* **53,** 152–172 (1984).
20. J. Lighthill, *Waves in Fluids.* Cambridge University Press, Cambridge (1978).
21. J. S. Turner, *Buoyancy Effects in Fluids.* Cambridge University Press, Cambridge (1973).

CONVECTION DANS UNE CAVITE CARREE DIFFERENTIELLEMENT CHAUFFEE, AVEC UN COUVERCLE OSCILLANT DANS SON PLAN

Résumé—On étudie numériquement l'écoulement d'un fluide visqueux stratifié thermiquement dans un réservoir carré. L'écoulement est produit par des oscillations de torsion du couvercle. Une différence de température verticale stabilisatrice $(T_H - T_C)$ est appliquée sur les parois horizontales; les deux parois latérales verticales sont thermiquement isolées. Des solutions numériques sont obtenues dans l'approximation de Boussinesq pour les équations de Navier–Stokes dépendantes du temps. On dégage des particularités des champs thermiques et dynamiques pour un large domaine des trois paramètres: le nombre de Reynolds *Re*, le nombre de Grashof *Gr* et le rapport de fréquence ω'. Il y a une possibilité de résonance qui conduit à une intensification de l'écoulement et à une augmentation corrélative du transport convectif de chaleur. Des résultats de calculs ordonnés systématiquement montrent que l'existence de la résonance est vérifiée et on obtient un accroissement de transfert de chaleur pour des valeurs particulières de ω'.

KONVEKTION IN EINEM UNGLEICHMÄSSIG BEHEIZTEN, QUADRATISCHEN HOHLRAUM, DESSEN DECKEL TORSIONSSCHWINGUNGEN AUSFÜHRT

Zusammenfassung—Die Strömung eines viskosen, thermisch geschichteten Fluids in einem quadratischen Hohlraum wird numerisch untersucht. Sie wird vom Deckel des Hohlraums angetrieben, welcher Torsionsschwingungen ausführt. Durch die obere und untere begrenzende Wand wird eine stabilisierende senkrechte Temperaturdifferenz $(T_H - T_C)$ aufgeprägt; die beiden senkrechten Seitenwände sind wärmegedämmt. Den numerischen Berechnungen liegen die instationären Navier–Stokes-Gleichungen mit der Boussinesq-Näherung zugrunde. Das Strömungs- und das Temperaturfeld wird für einen weiten Bereich der drei grundlegenden Parameter dargestellt: Reynolds-Zahl *Re*, Grashof-Zahl *Gr* und Frequenzverhältnis ω'. Von besonderem Interesse ist die Möglichkeit einer Resonanz. Dies führt zu einer Intensivierung der Strömung im Inneren und dadurch zu einer Verstärkung des konvektiven Wärmetransports. Systematisch durchgeführte Berechnungen weisen das Auftreten einer Resonanz nach, außerdem die damit verbundene Erhöhung des Wärmetransports für bestimmte Werte von ω'.

КОНВЕКЦИЯ В НЕГРЕВАЕМОЙ КВАДРАТНОЙ ПОЛОСТИ С ТОРСИОННО КОЛЕБЛЮЩЕЙСЯ КРЫШКОЙ

Аннотация—Численно исследуется течение вязкой жидкости с тепловой стратификацией в контейнере квадратного сечения. Течение вызывается торсионными колебаниями верхней крышки контейнера. На горизонтальные ограничивающие стенки налагается стабилизирующая вертикальная разность температур $(T_H - T_C)$; две вертикальные боковые стенки являются термически изолированными. Получены численные решения нестационарных уравнений Навье–Стокса в приближении Буссинеска. Приводятся характеристики нестационарного течения и тепловых полей для широких диапазонов измерений терх основных параметров: числа Рейнольдса *Re*, числа Грасгофа *Gr*, и отношения частот ω'. Особый интерес представляет возможность резонанса, что приводит к интенсификации течений в полости и связанному с ней увеличению конвективного теплопереноса. Наличие резонанса подтверждается систематизированными результатами расчетов; показано, что при определенных значениях ω' имеет место увеличение теплопереноса.